

Cyclic Bend Fatigue Reliability Investigation for Sn-Ag-Cu Solder Joints

F.X. Che*¹, H.L.J. Pang², W.H. Zhu¹ and Anthony Y. S. Sun¹

¹ United Test & Assembly Center Ltd. (UTAC)

Packaging Analysis & Design Center

5 Serangoon North Ave 5, Singapore 554916

*Email: FX_Che@sg.utacgroup.com, Tel: 65511345

² School of Mechanical and Aerospace Engineering, Nanyang Technological University

50 Nanyang Avenue, Singapore 639798

Abstract

In this study, VQFN assembly and FBGA assembly with Sn-3.8Ag-0.7Cu lead-free solder and OSP board surface finish were tested under four-point cyclic bending load at high temperature (125°C). Experimental results shows that the FBGA component has higher bending fatigue resistance compared to VQFN component at the same bending condition. Failure mode analysis shows that the dominant failure is solder joint fatigue cracking failure for both assemblies. FEA modeling and simulation were performed to investigate the stress-strain behavior of solder joint. Energy-based bending fatigue model has been developed based on experimental data and FEA results for VQFN assembly under high temperature bending condition. Bend fatigue model proposed in this paper for VQFN assembly was compared to energy-based fatigue model derived from bulk solder fatigue test. Bending fatigue model from VQFN specimen results in significant difference in predicting bending fatigue for FBGA assembly compared to experimental result. However, the fatigue model from bulk solder fatigue test is suitable for prediction of FBGA bending fatigue life.

1. Introduction

Board bending loading is encountered in board-level keypad loading test and electrical in circuit tests on printed circuit boards. Three-point and four-point cyclic bend tests may be used to study bending induced loading on solder joints of board assemblies. The correlation between three-point and four-point bend tests has been developed by Che and Pang [1-2]. Four-point bending test is widely used because it is suitable for testing large sample size of packages at similar loading condition (bending moments) between the inner load span regions. All the existing bend tests from reported literature [3-5] were conducted at room temperature (25°C) and were for tin-lead (Sn-Pb) solder joints. Typical thermal cycling reliability test from -40°C to 125°C was commonly used in industries and research areas to investigate the thermal fatigue reliability for soldered electronic assembly. Therefore, the bending test at 125°C is needed to study the bend fatigue reliability at elevated homologous temperatures. In this study, 7mm×7mm VQFN (48 I/Os) assembly and 15mm×15mm FBGA (324 I/Os) assembly with Sn-3.8Ag-0.7Cu lead-free solder and OSP board surface finish were tested under four-point cyclic bending load at high temperature (125°C). Bending fatigue reliability test comparison between VQFN and FBGA was presented and failure analysis was also carried out for them.

In this study, FEA modeling and simulation were also performed for different testing conditions and packages to

investigate the stress-strain behavior of solder joint. Elastic-Plastic-Creep (EPC) constitutive model was implemented in simulation using ANSYS FEA software to investigate the solder joint stress strain response under cyclic bending. Firstly, two-level submodeling method and one-level submodeling method were compared considering monotonic bending load. Fatigue models were developed for VQFN assembly with Sn-Ag-Cu lead free solder subjected to cyclic bending load at 125°C based on FEA results and fatigue test data using strain energy density as a fatigue damage parameter. Comparison the bend fatigue model created in this paper for VQFN assembly with the energy-based fatigue model [6] derived from bulk solder fatigue test is made to investigate the differences between fatigue data generated from bulk solder fatigue tests and cyclic bend tests.

2. Cyclic Bending Reliability Test

VQFN (Very thin Quad Flat No lead package) and FBGA (Fine pitch Ball Grid Array) with Sn-Ag-Cu solder and OSP board finish were selected for cyclic bend test. The specimen size as shown in Fig. 1 follows JEDEC standards [7-8]. VQFN package with geometry size of 7mm×7mm×0.8mm was mounted on the FR-4 PCB board of 132mm×77mm×1mm by 48 Sn-3.8Ag-0.7Cu solder joints with 0.1mm thickness. Silicon die in VQFN has the size of 3mm×3mm×0.254mm. The 15mm×15mm×1.0mm FBGA containing 324 solder balls with pitch of 0.8mm, 0.3mm solder height and the solder ball size of 0.4mm (before reflow) was used. One daisy chain loop containing all solder joints was designed for each component to take in-situ resistance measurement. The failure event was detected when resistance greater than 300 ohms lasting for 0.1second or longer. The support span of 100mm and load span of 70mm were used for four-point bend test. Constant bending moment can be obtained between load head in four-point bend test as shown in Fig. 2 so that all the samples within the load span are subjected to the same stress level (bending moment or curvature), which significantly increase the sample size. In this study, four-point cyclic bend tests with frequency of 1Hz were conducted for lead-free specimen at high temperature of 125°C. Table 1 shows the test matrix. The Minimum deflection was selected as 20% of maximum deflection. Four testing conditions were chosen for VQFN assembly in order to develop the bending fatigue model at 125°C, and one testing condition was chosen for FBGA assembly in order to compare bending reliability between FBGA and VQFN assemblies.

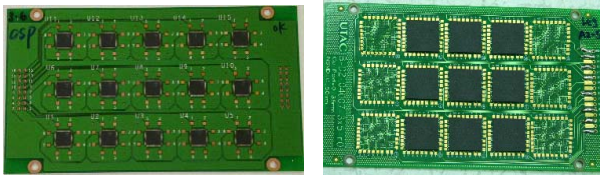


Fig. 1 Layout of specimens

Table I Test matrix for bending tests

Specimens	VQFN	VQFN	VQFN	VQFN	FBGA
Deflection (mm)	1.0	1.25	1.5	2.16	1.5

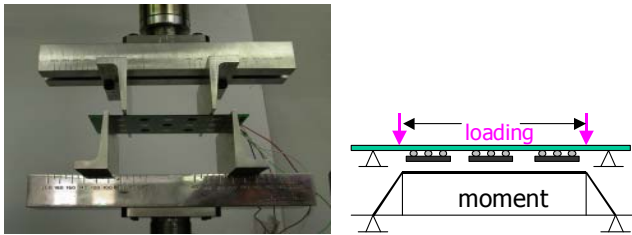


Fig. 2 Bending test setup

3. Experimental Result and Discussion

Fig. 3 shows the Weibull plots of cycle to failure for VQFN assembly under bend tests at 125°C. It can be seen that failure data satisfy the Weibull distribution very well. The cycle to failure increases significantly with displacement range decreasing. However, Weibull slopes of all test conditions have similar value, which indicating similar bending failure mode and mechanism for different bending loadings. It was shown by failure mode analysis using cross-section and microscopy as shown in Fig. 4 that failure mode exhibit solder fatigue failure with crack site close to solder/pad interface. Our research [2, 9] also showed that the acceleration factor of cycle to failure due to high temperature effect (125°C vs. 25°C) is around 4 to 7 times as compared to room temperature case with the same bending deflection.

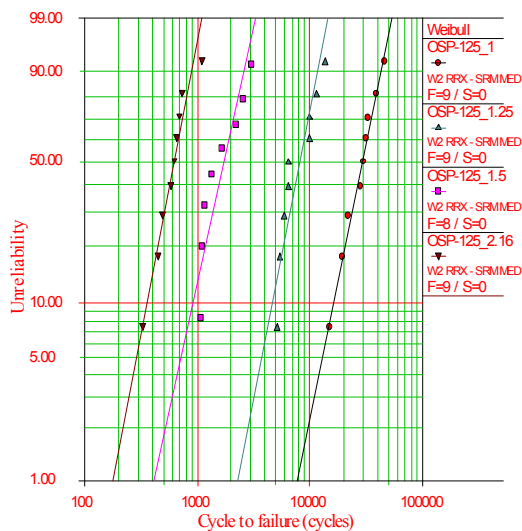


Fig. 3 Weibull plot of cycle to failure for VQFN assembly

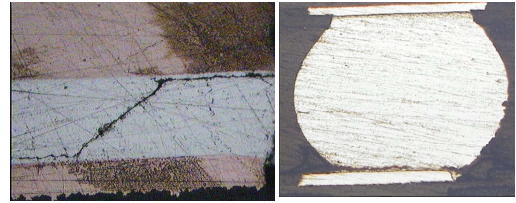


Fig. 4 Solder joint failure for VQFN and FBGA assembly

Fig. 5 shows the bending fatigue result comparison between VQFN and FBGA assembly subjected to the same bending load. The testing result in Fig. 5 shows that the bending cycle to failure for FBGA is about 10 times as that for VQFN under the same loading condition due to larger solder stand-off height of FBGA. The same failure mode of solder fatigue cracking failure as shown in Fig. 4 was observed for both VQFN and FBGA. Weibull parameters and failure data were summarized in Table 2. The MTTF is almost the same as averaged fatigue life. The Weibull slope for VQFN assembly is around 3 for different testing conditions. However, the Weibull slope of 6.5 for FBGA is higher than that for VQFN.

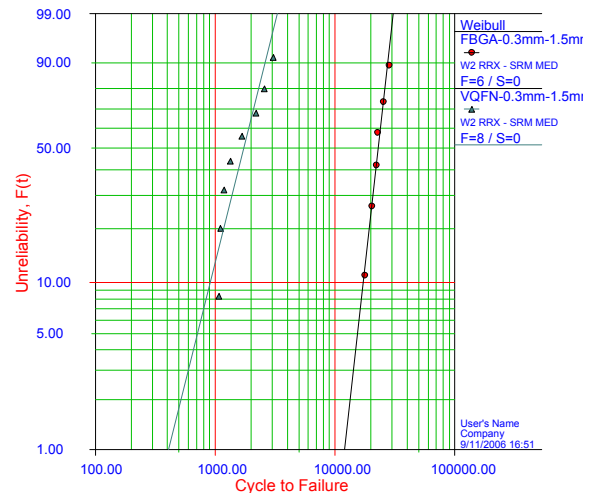


Fig. 5 Weibull plot comparison between FBGA and VQFN

Table II Summary of failure data for all bend tests

Test conditions	Solpe	Char. life	MTTF	Ave. life
VQFN_2.16mm	3.38	699	628	631
VQFN_1.5mm	2.93	1968	1756	1778
VQFN_1.25mm	3.30	9185	8239	8331
VQFN_1.0mm	3.15	32949	29488	29455
FBGA_1.5mm	6.54	24391	22735	22849

4. FEA Study for Bending Fatigue Test

4.1 Submodeling method validation

FEA modeling for bend fatigue tests were conducted to investigate the stress strain behavior of solder joint. Conventional 3D FEA model for board-level simulation is not desirable due to larger element size and high-level computing resource requirement. Therefore, submodeling technique is a desirable choice. Firstly, two-level submodeling and one-level submodeling were compared in order to investigate mesh

effect on FEA results. One is called two-level submodeling method as shown in Fig. 6 where the global board-level quarter model was solved firstly. Then DOF results were transferred and interpolated to cut boundary in first package-level submodel with medium mesh. Finally, the DOF results from first-level submodel were transferred and interpolated to cut boundary in second-level submodel with fine mesh. In two-level submodeling method, the package-level FEA model is a transitional model, which is a submodel relative to the board-level global model while it becomes the package-level global model relative to second-level submodel. This method can satisfy requirement of elements transferring from coarser mesh to finer mesh. It was expected that two-level submodeling method leads to more accurate results but complicated procedure is needed due to twice DOF interpolations. The other method is called one-level or traditional submodeling as shown in Fig. 7. In this method, global model and submodel are the same as board-level global model and second-level submodel used in two-level submodeling method, respectively. The DOF results from global model were transferred to final submodel directly without using package-level submodel as transitional model. However, it maybe give arise to more error because DOF results were interpolated and transferred from too coarse mesh in board-level global model to finer mesh in submodel. In this study, these two submodeling methods were performed to find a desirable method. For convenience, the monotonic four-point bending load was used in this validation procedure. Validation will be done by comparing numerical results from different modeling method.

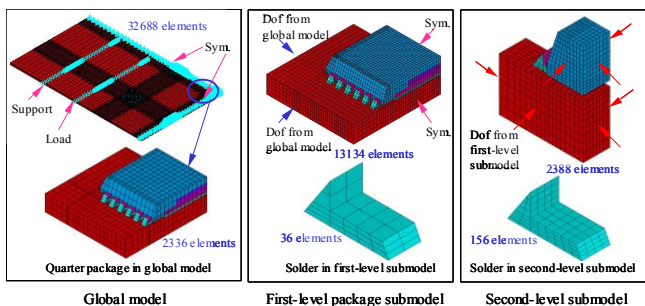


Fig. 6 Two-level submodeling method

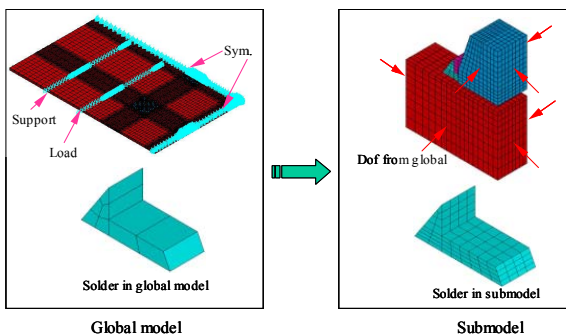


Fig. 7 One-level submodeling method

The displacement range from zero to 6mm was added on loading position of global model in 1 second using 6 load steps in FEA simulation. Viscoplastic constitutive model for

solder material, multi-linear kinematic hardening plastic model for copper, and orthotropic elastic model for PCB were used in FEA model. Fig. 8 shows the volume-averaged plastic strain energy density at the last load step with displacement of 6mm for different models considering whole solder joint as averaging volume. It can be seen that one-level submodel and two-level submodel result in almost the same result. Therefore, one-level submodeling method is effective and sufficient for FEA modeling and simulation of VQFN assembly. Strain result from FEA modeling was also validated by comparing with experimental result by Che and Pang [2, 9].

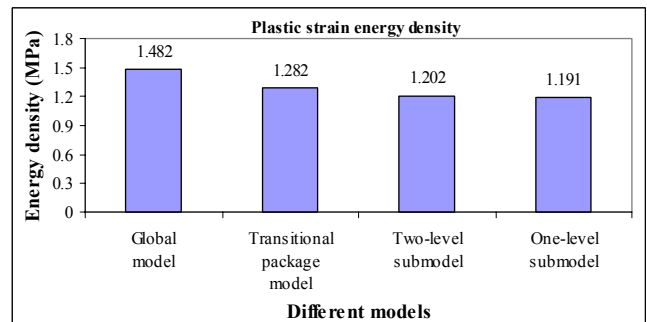


Fig. 8 Plastic strain energy density for different models

4.2 Bending fatigue model development for VQFN solder joint

For cyclic bending simulation, one concern is how to select one suitable solder constitutive model. Usually, the elastic-plastic-creep (EPC) model [10] was used for cyclic loading simulation from slow loading rate (thermal cycling) to fast loading rate (mechanical bending), while the viscoplastic Anand model is suitable for slow loading rate, such as thermal cycling. The effect of constitutive model on solder stress-strain behavior has been presented by Che et al. [9, 11] using FEA simulation method. The result showed that EPC model is one reasonable model for simulate high frequency cyclic bending load condition. It needs more than 15 simulation cycles to get the converged numerical result when using Anand model for solder material while the numerical result can be converged after 4 or 5 simulation cycles when using EPC model for solder material [3, 9, 11]. Therefore, in the subsequent bending simulation, the EPC model for solder was used.

Based on limited literature [3-5], bending fatigue model for Sn-Ag-Cu solder was not documented. In this section, bending fatigue models were presented for VQFN with Sn-Ag-Cu solder at high temperature of 125°C. Strain energy density was selected as damage parameter because it is a comprehensive factor considering both stress and strain effects. The critical solder joint can be found to be located at component corner from global model result, and then the submodel was established based on this critical solder joint location. Typically, the volume-averaged method is used to output the simulation result for fatigue life evaluation. The top and bottom solder joint interface layers were selected for volume-averaged strain energy density calculation as shown in Fig. 9 The simulation result shows that the accumulated strain

energy density on bottom layer is much higher than that on top layer due to bending effect of PCB. Therefore, the subsequent analysis will focus on bottom layer volume-averaged result.

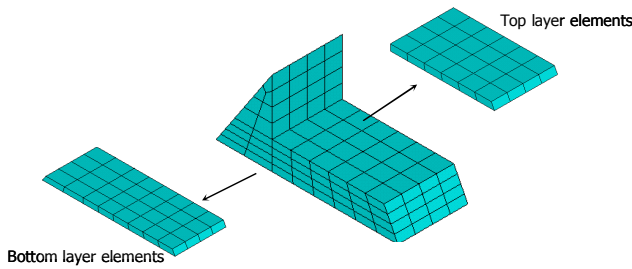


Fig. 9 Volume-averaged elements

The inelastic strain energy density results were given in Table 3 for different simulation conditions. Combining FEA results in Table 3 and experimental fatigue life results (MTTF) in Table 2, the bending fatigue model can be achieved. Fig. 10 shows the relationship of MTTF and inelastic strain energy density for bend test. The power law function can fit data well. The energy-based bending fatigue model can be developed as follows:

$$N_f = 34.28(\Delta W)^{-0.907} \quad (1)$$

where ΔW , are inelastic strain energy density accumulation per cycle.

Table III Inelastic energy density (MPa) from FEA result

Displacement	1mm	1.25mm	1.5mm	2.16mm
Energy density (Mpa)	6.20e-4	2.57e-3	9.60e-3	4.80e-2

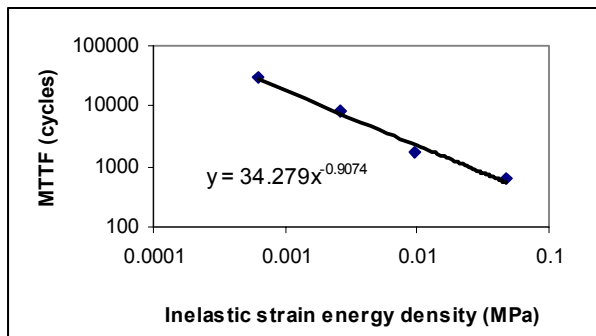


Fig. 10 Bending fatigue model for VQFN Sn-Ag-Cu solder

4.3 FEA analysis for FBGA assembly

Submodeling method was also implemented for FBGA bending simulation. Fig. 11 shows the quarter global model and corresponding submodel. The bending displacement from 0.3mm to 1.5mm was applied on FBGA with support span of 100mm and loading span of 70mm. The EPC model was used for solder material. Morrow's energy-based model is used for bending fatigue life prediction [6]:

$$N_f^n W_p = A \quad (2)$$

The fatigue ductility coefficient, A , and the fatigue exponent, n , can be obtained from fatigue test data analysis. In

order to simulate bending fatigue at 125°C with frequency of 1 Hz, the isothermal fatigue test condition for bulk solder material is selected as the same condition as bending test. The material constants n , and A for Sn-3.8Ag-0.7Cu solder are 0.953, and 1492.8MPa, respectively [6]. The volume-averaged energy density can be extracted from FEA result. Three different averaged volumes were developed for thermal cycling fatigue life prediction of PBGA by Che et al. [12, 13] and results showed that selecting outermost ring elements for calculating volume-averaged energy density could predict more accurate fatigue life. In this study for FBGA bending fatigue life prediction, these three volumes as shown in Fig. 12 were also considered, i.e. whole interface layer, outer two rings and outermost ring. Fig. 13 shows the predicted bending fatigue life for FBGA assembly using different averaging volumes. It can be seen that using whole interface layer elements as averaging volume overestimates the bending fatigue life of FBGA and using elements within outer two rings and outermost ring as averaging volume can predict reasonable and accurate bending fatigue life compared to experimental result. Therefore, for BGA type assembly, the outer ring volume-averaged method is proper in fatigue life prediction for both thermal cycling and cyclic bending load conditions. In addition, the fatigue model of equation (1) from VQFN was also used to predict bending fatigue life of FBGA. The results show that equation (1) underestimates the bending fatigue life of FBGA significantly compared to experimental result. It seems that equation (1) is just suitable for predicting bending fatigue life of VQFN. The reason for this problem is that fatigue crack initiation site or propagation path is different for VQFN and FBGA structure. The crack propagation for VQFN will be faster than FBGA due to thinner solder joint layer and peripheral solder distribution structure for VQFN. The further study should be carried out for bending fatigue comparison between QFN and BGA packages.

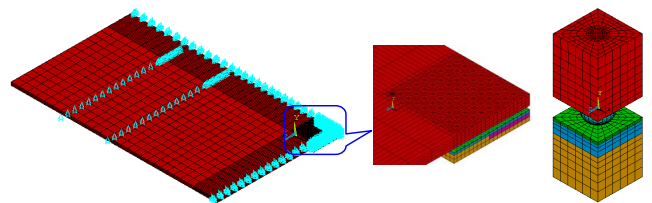


Fig. 11 Global FBGA model and submodel

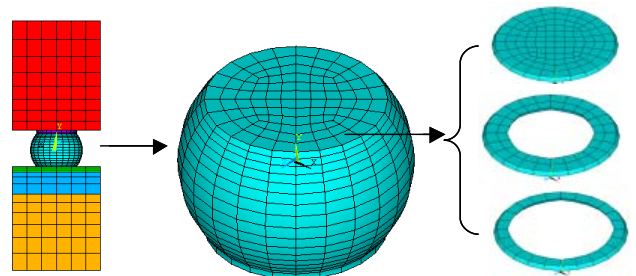


Fig. 12 Volume selection for volume-averaged method

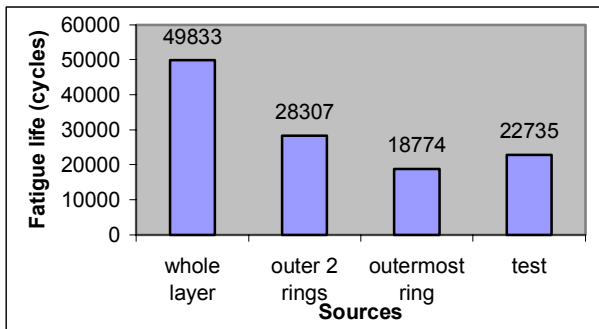


Fig. 13 Bending fatigue life prediction results for FBGA

5. Conclusions

Bending fatigue tests were conducted for VQFN and FBGA assemblies at 125°C. The cycle to failure increases significantly with displacement ranges decreasing. The bending cycle to failure for FBGA is about 10 times as that for VQFN under the same loading condition. However, the same failure mode of solder fatigue cracking failure was observed for both VQFN and FBGA assemblies. Place conclusions here.

FEA modeling and simulation were performed for different testing conditions. One-level and two-level submodeling methods were compared. It was shown that one-level submodeling method is effective and sufficient for FEA simulation. Bending fatigue life model was developed for VQFN assembly subjected to cyclic bending load at 125°C. The bending fatigue life prediction methodology for FBGA was presented. The outer ring volume-averaged method is proper in bending fatigue life prediction for BGA type assembly.

References

1. Che, F.X. and Pang, H.L.J., "Bend Fatigue Reliability Test and Analysis for Pb-Free Solder Joint", *Proceedings of 7th EPTC*, Singapore, December, 2005, pp.868-872.
2. Pang, H.L.J. and Che, F.X., "Isothermal Cyclic Bend Fatigue Test Method for Lead Free Solder Joints", *Proceedings of 2006 Inter Society Conference on Thermal Phenomena*, San Diego, California, May 30-June 2, 2006, pp.1011-1017.
3. Shetty, S., Lehtinen, V., Dasgupta, A., et al., "Fatigue of Chip Scale Package Interconnects Due to Cyclic Bending", *Journal of Electronic Packaging*, Vol. 123 (2001), pp.302-308.
4. Mercado, L.L., Philips, B., Sahasrabudhe, S., et al., "Use-Condition-Based Cyclic Bend Test Development for Handheld Components", *Proceedings of 54th Electronic Components and Technology Conference*, Las Vegas, June 1-4, 2004, pp.1279-1287.
5. Geng, P., Chen, P. and Ling, Y., "Effect of Strain Rate on Solder Joint Failure under Mechanical Load", *Proceedings of 52nd Electronic Components and Technology Conference*, 2002, pp.974-978.
6. Pang, J.H.L., Xiong, B.S. and Low, T.H., "Creep and Fatigue Characterization of Lead Free 95.5Sn-3.8Ag-0.7Cu solder", *Proceedings of 54th Electronic Components*

- and Technology Conference, Las Vegas, June 1-4, 2004, pp.1333-1337.
7. JEDEC Standard, JESD22-B111: *Board Level Drop Test Method of Components for Handheld Electronic Products*, 2003.
8. JEDEC Standard, IPC/JEDEC-9702: *Monotonic Bend Characterization of Board-Level Interconnects*, 2004.
9. Che, F.X. and Pang, J.H.L., "Modeling Board-Level Four-Point Bend Fatigue and Impact Drop Tests", *Proceedings of 56th Electronic Components and Technology Conference*, San Diego, California, May 30-June 2, 2006, pp.443-448.
10. Pang, H.L.J., Chong, D.Y.R. and Low, T.H., "Thermal Cycling Analysis of Flip-Chip Solder Joint Reliability", *IEEE Transaction on Components and Packaging Technologies*, Vol. 24, No.4 (2001), pp.705-712.
11. Che, F.X., Pang, J.H.L., Zhu, W. H., Sun, W. and Sun, Y. S., "Modeling Constitutive Model Effect on Reliability of Lead-Free Solder Joints", *Proceedings of ICEPT2006*, Shanghai, China, Aug. 27-29, 2006, pp.155-160.
12. Che, F.X. and Pang, H.L.J., "Thermal Fatigue Reliability Analysis for PBGA with Sn-3.8Ag-0.7Cu Solder Joints", *Proceedings of 6th EPTC*, Singapore, December, 2004, pp.787-792.
13. Che, F. X., Pang, H.L.J., Xiong, B.C., Xu, L.H. and Low, T.H., "Lead Free Solder Joint Reliability Characterization for PBGA, PQFP and TSSOP Assemblies", *Proceedings of 56th Electronic Components and Technology Conference*, Florida, May 31-June 3, 2005, pp.916-921.